IMPEDANCE STUDIES ON THE ELECTROSTATIC SEPARATORS

N. Wang*, Y.Z. Liu, Y.D. Liu, S.K. Tian, B. Chen
Institute of High Energy Physics, CAS, Beijing, China
University of Chinese Academy of Sciences, Beijing, China

Abstract

Electrostatic separator is a crucial component required in the future high energy circular electron position colliders to separate electron and positron beams, therefore the two beams can be separated, either to avoid beam collision at certain locations or share the RF cavities at high beam operation energies. The impedance contribution from the component is one of the main concerns during the design of the electrostatic separators. In this paper, the impedance characteristic of the electrostatic separator is investigated systematically. The transverse higher order modes trapped in the component is examined by simulations. The mitigation of the trapped modes is also explored.

INTRODUCTION

Electrostatic separators have been used extensively in the 19th century in electron positron colliders to generate closed orbit displacements of opposite sign depending on the charge of the stored beams. So that parasitic collisions can be avoided outside the experimental detector. This scheme allows multiple bunches of electrons and positrons to be stored when the two beams sharing the vacuum chamber, thereby increasing the luminosity, such as in LEP [1], BEPC [2], and CESR [3], etc. Nowadays, along with the development of the future high energy electron positron colliders, the wide operating beam energy range required quite different RF voltages. In order to save the number of cavities at top energies, the sharing scheme of RF cavities in both rings were proposed in the Circular Electron Positron Collider (CEPC) [4]. The electrostatic separators, combined with dipole magnets are utilized to provide both electric and magnetic fields in order to assure both beams pass through the centre of RF cavities, while avoiding synchrotron light hits the cavities. For the incoming beam, the electric and magnetic forces cancel each other, leaving the beam undeflected. For the outgoing beam, the electric and magnetic forces act in the same direction, yielding a doubled deflecting force. In CEPC, 40 separators are requried and located symmetrically at both ends of the RF regions. During Higgs mode, all RF cavities are shared by the electron and positron beams. For the W and Z modes, the separators in the RF region are turned off so that all bunches can be filled around the entire electron and positron rings.

The electrostatic separators show several impedance effects that may degrade the machine performance. First, the parasitic beam power loss in the components can cause heating of the electrodes, which may further induce increased outgassing and thus provoke a significant rise in pressure [1]. Besides, they have been important contributors to the overall impedance and the RF fields generated during the beam passage can also degrade the high voltage performance. Recent studies in CEPC show that the transverse trapped modes in the component are important contributors to the coupled bunch instabilities at the Z-pole operation mode [5].

In the following, the design features and impedance characteristics of the electrostatic separator are introduced. Then the properties of the transverse trapped modes and their influence to the beam are presented, followed by an investigation of potential mitigation strategies. Finally, conclusions are drawn.

DESIGN FEATURES

The electrostatic separator consists of a pair of Titanium parallel electrodes mounted in a stainless steel vacuum tank [6]. Each electrode is supported by two metal-ceramic supports, which insulate the electrode from the vacuum tank, therefore the electrode can be charged to its desired voltage via high voltage feedthroughs situated at the extremities of the electrode.

Each electrostatic separator has an effective length of 4 m and a design electric field strength of 2 MV/m. The two electrodes are biased with equal magnitude but opposite polarities of high voltage. The separation between the two parallel electrodes is 75 mm. The cross section of the electrodes are optimized with bump edges to improve the field homogeneity. In order to decrease the beam coupling impedance, the ground plates are introduced on the side wall of the vacuum chamber and tapering ends are adopted between the vacuum tank and beam pipe. To further mitigate the thermal effects from the beam parasitic power loss dissipated on the electrodes, cooling loops are adopted on the back of the high voltage electrodes.

The longitudinal cross section of the simplified model used in the wakefield simulations is shown in Fig. 1. The green plates show the two parallel electrodes located vertically. The yellow slot shows one of the two ground plates settled between the electrodes. They are supposed to provide smooth path for the image current and to mitigate the interruption introduced by the electrodes. Taper transitions are designed at both ends of the vacuum tank and the ground plates to provide smooth transition to the nominal beam pipe.

IMPEDANCE CHARACTERISTICS

The longitudinal and transverse impedances are simulated with CST [7] wakefield solver taking a Gaussian excitation beam with rms bunch length of 6 mm. The real and imagi-

* wangn@ihep.ac.cn

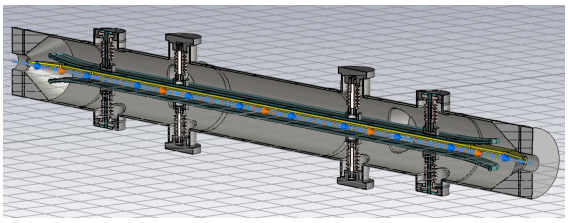

Figure 1: Simplified model of the electrostatic separator used in the wakefield simulations.

nary part of the longitudinal impedance is shown in Fig. 2. The narrowband impedances are mainly locate below 4 GHz, with two dominant resonances at 137 MHz and 734 MHz. Here, it should be noted that the wake field has not fully converged, consequently, the amplitude of the resonances are not accurate. Further Eigenmode simulations demonstrate that longitudinal narrowband impedance is not a critical concern for the CEPC beam.

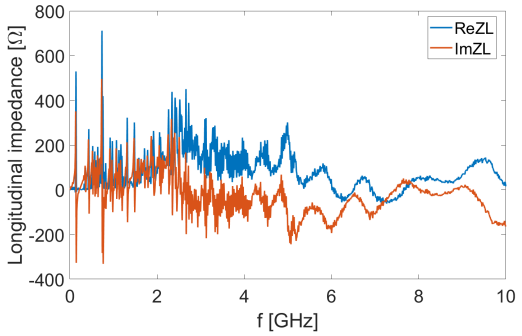

Figure 2: Longitudinal impedance of the electrostatic separator.

The real and imaginary parts of the horizontal impedance are presented in Fig. 3. There are two dominant resonant peaks at frequencies of 138 MHz and 3.2 GHz. The wakefield still fails to reach full convergence after tracking the wakefield for 10 m long. The characteristics of the transverse trapped modes will be discussed in detail in the following sections.

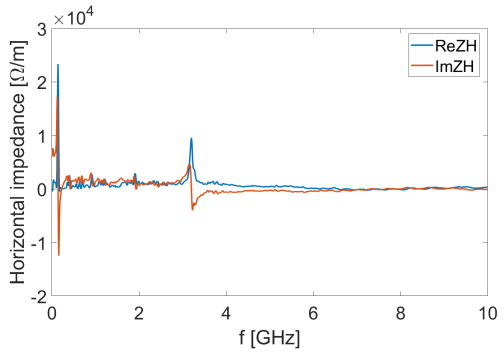

Figure 3: Horizontal impedance of the electrostatic separator.

The longitudinal and transverse broadband impedance are evaluated and compared with the total impedance budget [8]. When accounting for contributions from all electrostatic separators, their total contributions to both longitudinal and transverse broadband impedance are each less than 1%, which are expected to exert no prominent influence to the single bunch beam dynamics.

Another important concern is the parasitic beam power loss dissipation inside the structure during the beam passage, particularly for the Z operation mode. The total beam power loss can be evaluated by the loss factor. At the nominal bunch current of 803.5 mA and a bunch number of 11934, the rms bunch lengths are 6.0 mm and 8.7 mm for the case with only longitudinal impedance and the case with both impedance and beam-beam interaction, respectively. The loss factor is evaluated with the specific bunch length in wakefield simulations. With single beam and only impedance bunch lengthening, the loss factor is 0.74 V/pC and the total beam power loss is 13 kW. The power loss dissipation on different components inside the separator are shown in Fig. 4. For the nominal filling pattern, the total power loss dissipated on the electrodes amounts to approximately 850 W.

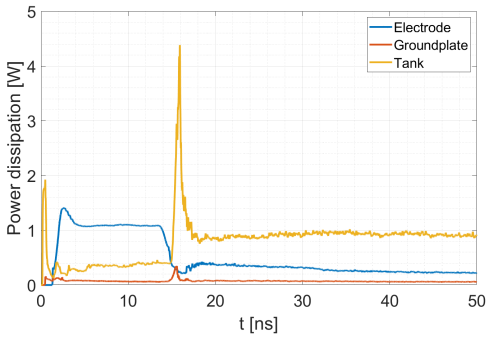

Figure 4: Power loss dissipation on different parts of the electrostatic separator.

For the case with collision, the bunch length will be further increased and the loss factor is decreased to 0.61 V/pC. However, both electron and positron beams will loss beam energies inside the structure. Therefore, the total beam power loss is doubled to be 22 kW. Roughly scales give the power loss dissipated on the electrodes in the Z collision mode is approximately 1.4 kW. A cooling system is designed for the electrodes to avoid any heating damages.

TRANSVERSE TRAPPED MODES

The HOMs at low frequencies are simulated using the CST Eigenmode Solver. All the longitudinal HOMs are well below the coupled-bunch instability threshold defined by synchrotron radiation damping. Nevertheless, several transverse modes exceed the threshold at the Z operation mode. Meanwhile, four dominant modes below 100 MHz exceed the instability threshold in the W operation mode. Here, it is assumed that the HOM spectra of different separators overlap with each other.

The transverse modes can be effectively damped when the feedthroughs are terminated with waveguide ports, which means perfect matching and no field reflections at the terminations of the feedthroughs. The amplitude of the horizontal modes with different terminations on the feedthroughs are

shown in Fig. 5 and compared with coupled bunch instability thresholds for different cases. However, achieving perfect impedance matching at the feedthrough terminations is challenging under high-voltage operation. Therefore, improved matching at the feedthrough ends is preferred, and additional damping of trapped modes is also considered in the following section.

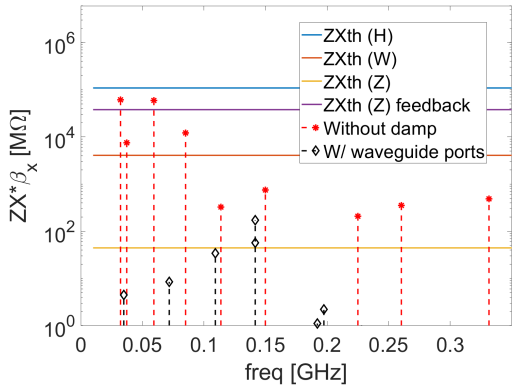

Figure 5: Horizontal HOMs of the electrostatic separator with electric boundary or waveguide ports at the terminal of the feedthroughs.

MITIGATION OF TRANSVERSE MODES

Mitigation of the horizontal modes are investigated when the feedthroughs are terminated with electric boundaries. Eigenmode simulations show the most dominant horizontal modes at 32.4 MHz, 59.6 MHz, 84.8 MHz and 91.0 MHz. The electromagnetic field distribution of the first horizontal mode is shown in Fig. 6. The field is concentrated between the electrodes, as well as around the feedthroughs and supports, which closely resembles the rigid waveguide modes observed in the in vacuum undulators [9, 10]. Therefore, mode mitigation using absorbing materials placed around the feedthoughs and the ceramic supports is proposed. For the absorbing material selection, SiC is adopted to avoid magnetic field degradation induced by magnetic materials such as ferrite. The permeability and permittivity of the absorber used in the following simulations are shown in Fig. 7.

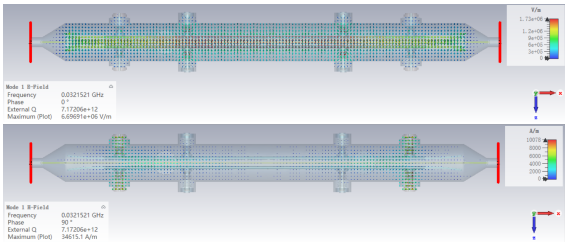

Figure 6: The electric and magnetic field distributions of the horizontal mode at 32.4 MHz.

By adding absorbing materials at the ceramic support, or directly change the material of the ceramic support or the feedthroughs, the shunt impedance of the first few dominant modes are simulated and shown in Fig. 8. The results

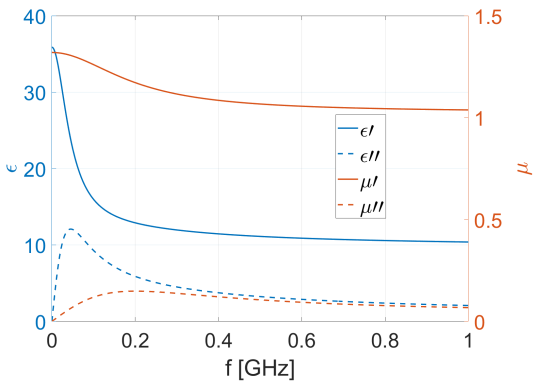

Figure 7: Permeability and permittivity of SiC used for mode damping in the electrostatic separator.

demonstrate that all adopted damping schemes effectively suppress the HOMs, with the amplitudes of the dominant HOMs reduced by approximately one order of magnitude.

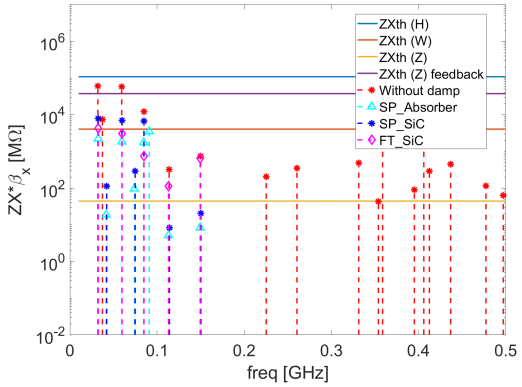

Figure 8: Horizontal HOMs of the electrostatic separator considering different damping strategies.

CONCLUSION

The impedance-related characteristics of the separators are primarily investigated, with a focus on their performance in the Z operating mode. The key impedance features include abundant higher-order modes and significant beam power loss. The HOMs are dependent on the termination of the feedthroughs. For an poor matching at the termination, it can excite coupled-bunch instabilities, therefore mitigation strategies by adding absorbing materials are considered and proved to be effective in damping the modes. On the other hand, the beam power loss can lead to additional heat deposition on the electrodes. The power loss on the electrodes are estimated to be 850 W for single beam and 1.4 kW for colliding beams. To mitigate such thermal effects, a water cooling scheme is adopted in the mechanical design.

REFERENCES

[1] W. Kalbreier, N. Garrel, M. Laffin, V. Mertens, G. Rogner, and G. von Holtey, "Commissioning and operating experience with the electrostatic beam separation system of the LEP e+e-

collider", in *Proc. EPAC'90*, Nice, France, pp. 815–818, Jun. 1990. https://cds.cern.ch/record/210129

[2] J. Q. Wang, "Impedance of the BEPCII electrostatic separators", in *Proc. APAC'01*, Beijing, China, paper WEP072, Sep. 2001. https://accelconf.web.cern.ch/a01/PDF/WEP072.pdf

[3] A. Temnykh, "The CESR horizontal separators impedance study", in *Proc. PAC'01*, Chicago, IL, USA, paper RPPH099, Jun. 2001.

[4] J. Gao, "CEPC technical design report: accelerator", *Radiat. Detect. Technol. Methods*, vol. 8, no. 1, pp. 1–1105, 2024. doi:10.1007/s41605-024-00463-y

[5] N. Wang, Y. Zhang, H. S. Xu, S. K. Tian, Y. D. Liu, and C. T. Lin, "Single beam collective effects at CEPC", Presented at eeFACT'25, Tsukuba, Japan, paper WG4-31, Mar. 2025. https://indico.jacow.org/event/75/contributions/6857/

[6] J. B. Zhu *et al.*, "Study of electrostatic-magnetic deflector for cepc", *Radiat. Detect. Technol. Methods*, vol. 5, pp. 347–355, 2021. doi:10.1007/s41605-021-00261-w

[7] "CST Studio Suite", https://www.cst.com,

[8] N. Wang, "Impedance driven collective effects in CEPC", *J. Instrum.*, vol. 19, p. P02016, 2024. doi:10.1088/1748-0221/19/02/P02016

[9] K. Tian, J. J. Sebek, A. D. Ringwall, and Z. Li, "Damping trapped modes in an in-vacuum undulator at a Synchrotron Radiation Light Source", *Phys. Rev. Accel. Beams*, vol. 22, p. 050702, 2019. doi:10.1103/PhysRevAccelBeams.22.050702

[10] N. Wang *et al.*, "Impedance characterization and optimization of the High Energy Photon Source in-vacuum undulator", *Phys. Rev. Accel. Beams*, vol. 28, p. 094401, 2025. doi:10.1103/ztx5-848v